Geomechanics and Engineering, *Vol. 35, No. 6 (2023) 647-663*
https://doi.org/10.12989/gae.2023.35.6.647

Prediction of TBM disc cutter wear based on field parameters regression analysis

Lei She[1], Yan-long Li*[1], Chao Wang[2], She-rong Zhang[2], Sun-wen He[3], Wen-jie Liu[2], Min Du[2] and Shi-min Li[3]

[1]*State Key Laboratory of Eco-Hydraulics in Northwest Arid Region of China, Xi'an University of Technology, No. 5 South Jinhua Road, Xi'an 710048, China*
[2]*School of Civil Engineering, Tianjin University, No. 135 Yaguan Road, Tianjin 300072, China*
[3]*Power China Co., Ltd., No. 22 West Chegongzhuang Road, Beijing 100048, China*

(*Received July 4, 2023, Revised November 24, 2023, Accepted November 28, 2023*)

Abstract. The investigation of the disc cutter wear prediction has an important guiding role in TBM equipment selection, project planning, and cost forecasting, especially when tunneling in a long-distance rock formations with high strength and high abrasivity. In this study, a comprehensive database of disc cutter wear data, geological properties, and tunneling parameters is obtained from a 1326 m excavated metro tunnel project in leptynite in Shenzhen, China. The failure forms and wear consumption of disc cutters on site are analyzed with emphasis. The results showed that 81% of disc cutters fail due to uniform wear, and other cutters are replaced owing to abnormal wear, especially flat wear of the cutter rings. In addition, it is found that there is a reasonable direct proportional relationship between the uniform wear rate (*WR*) and the installation radius (*R*), and the coefficient depends on geological characteristics and tunneling parameters. Thus, a preliminary prediction formula of the uniform wear rate, based on the installation radius of the cutterhead, was established. The correlation between some important geological properties (K_V and *UCS*) along with some tunneling parameters (F_n and p) and wear rate was discussed using regression analysis methods, and several prediction models for uniform wear rate were developed. Compared with a single variable, the multivariable model shows better prediction ability, and 89% of *WR* can be accurately estimated. The prediction model has reliability and provides a practical tool for wear prediction of disc cutter under similar hard rock projects with similar geological conditions.

Keywords: disc cutter wear; failure analysis; geological properties; prediction model; tunneling parameters

1. Introduction

Tunnel boring machines (TBMs) have been popular in hard rock excavation projects due to their advantages of high excavation efficiency, low safety risks, and good construction quality (Liu *et al.* 2016, Sun *et al.* 2019, He *et al.* 2020). As the core component of the TBM, the disc cutter is located at the forefront of the excavation equipment and directly participates in the rock-breaking task. Owing to the complex geological environment and operating conditions, the disc cutter will inevitably wear and even become failure. However, mechanical accidents caused by excessive wear of disc cutters are quite common (Kim *et al.* 2020, Liu *et al.* 2017). Especially in some full section rock stratum TBM projects with high strength and high abrasivity, if the disc cutter is not replaced in time, the wear of the supporting tools will accelerate, which may trigger damage to the cutterhead components or cause the cutterhead to become stuck, resulting in a decline in the TBM tunneling performance (Jeon and Lee 2023). In addition, because disc cutters and support rings are expensive, frequent replacement of these components undoubtedly increases the cost of excavation (Yang *et al.* 2019). Therefore, it is of great significance to analyze and study the failure form and wear consumption of each disc cutter to check and replace the cutter, optimize the operation parameters and improve the tunneling efficiency.

To fully obtain the wear information of disc cutters, the main methods of inside-cutterhead inspection, online monitoring and wear prediction of disc cutters have been proposed (Lan *et al.* 2019, Wang *et al.* 2019, Karami *et al.* 2020). Frequent cutter stop inspection work, a complex detection environment, and expensive monitoring equipment will seriously reduce the utilization rate of TBMs and increase the construction cost (Sun *et al.* 2019, Li *et al.* 2019). Therefore, the practicability of the inside-cutterhead inspection and online monitoring method for engineering needs to be discussed.

Comparatively speaking, it is obviously more feasible and practical to establish a reliable disc cutter wear prediction method to evaluate cutter consumption and make maintenance plans before project construction. Based on reported research, cutter wear is a complex process involving multiple loads, such as extrusion, shear, and friction, and is mainly affected by geological conditions, cutter characteristic parameters, and mechanical excavation performance indicators (Gong *et al.* 2016, Yang *et al.* 2019, Zhang *et al.* 2021, She *et al.* 2022a, Li *et al.* 2023). The

*Corresponding author, Professor
E-mail: liyanlong@xaut.edu.cn

ISSN: 2005-307X (Print), 2092-6219 (Online)

existing cutter wear prediction models can be summarized into two categories:

(1) The empirical approach: This usually requires field borehole tests and special laboratory tests to obtain a large number of rock parameters and mechanical property parameters, and a series of modeling work is carried out using both simple and complex statistical analysis methods to obtain mathematical equations or relational models. The geological parameters involved include rock quality designation (RQD), uniaxial compressive strength (UCS), Cerchar abrasivity index (CAI), Norwegian abrasiveness value (AV), quartz content (Q), Vicker's hardness number (VHN), etc. (Bruland 1998; Gong *et al.* 2009; Hassanpour *et al.* 2011, 2014, Ko *et al.* 2016). The machine performance parameters include the cutterhead thrust (TF), cutterhead torque (TR), penetration rate (PR), and field penetration index (FPI) (Hassanpur *et al.* 2010, Lan *et al.* 2020). Additionally, some researchers have proposed prediction models of the cutter wear rate and cutting life based on the number of cutter changes and wear amount of disc cutters tracked in the field (Frenzel *et al.* 2011, Sun *et al.* 2019). The models developed at the Colorado School of Mines (CSM) (Rostami 1997) and Norwegian University of Science and Technology (NTNU) (Bruland 1998), as well as that proposed by Gehring (1995), are the most commonly used empirical models for estimating the wear rate.

(2) The semitheoretical approach: Different from the empirical approach, the semitheoretical approach is dedicated to the force analysis or friction energy theory of disc cutters to understand the micromechanism of cutter wear or the stress state of rock breakage from the perspective of cutter geometric motion and contact with rock (Ren *et al.* 2018, Shen *et al.* 2022). Based on this context, the prediction model of the cutter wear rate or cutting life is developed by using statistical analysis software. For example, Rostami (1997, 2013) proposed a force estimation equation for an approximately constant cross-section type cutter based on a large number of linear cutting tests and incorporated this equation into many cutter prediction models. Zhao *et al.* (2014) developed a disc cutter wear prediction model based on the abrasion wear mechanism and compared it with experimental results. Wang *et al*. (2015) established an energy method to predict cutter wear based on cutter force and cutter movement and calculated abrasive wear by the cutter friction work. Li *et al.* (2017) proposed several replacement measures for cutting tools in soft ground using the interval wear analysis method. Su *et al*. (2020) proposed a uniform wear prediction model for disc cutters by establishing the relative sliding distance equation for a single disc cutter. Furthermore, Yu *et al*. (2021) designed a new one-dimensional convolutional neural network mapping model, thus developing a real-time estimation method for disc cutter wear based on field parameters.

Although the abovementioned research work for cutter wear has been relatively fruitful, very limited work has been done to develop practical models for predicting cutter wear and the associated costs (She *et al.* 2022b, c). On the one hand, the existing prediction models involve a large amount of rock mass or intact rock information and excavation parameters, but considering the complexity and variability of engineering geological conditions in long-distance excavation projects, it is difficult to obtain more accurate information, and parameters such as CAI and AV can only be acquired by generating special tests, thus leading to the lack of accuracy and versatility of these models. On the other hand, due to the special spatial distribution of the cutterhead and cutters, the disc cutter installed in different positions will produce different rock breakage characteristics and wear states. However, the previously developed models predict the average life of disc cutters from the perspective of the whole cutterhead and then roughly estimate the wear of disc cutters at each cutter position according to the law of installation position. Obviously, this is always inconsistent with the real wear situation, which is not conducive to the formulation of a scheme in cutter maintenance and replacement. Consequently, it is most accurate to grasp the wear trend of each disc cutter by combining it with the engineering field tracking data.

This study is based on a long-distance rock tunnel excavation project with high strength and high abrasivity, aiming to offer a more practical and accurate estimation model for failure determination and wear evaluation of disc cutter in hard rock tunneling. In this study, a comprehensive database of geological information, tunneling parameters, and disc cutter wear data is collected from a metro tunnel project in Shenzhen, China. The disc cutter wear data at each installation position of the cutterhead are statistically analyzed, and the relationship between the common engineering rock mass parameters, tunneling parameters, and disc cutter wear is established.

2. Project overview

2.1 Site geological background

Shenzhen is located on the Pearl River Delta Plain on the south-central coast of Guangdong Province in southern China. Metro Line 12 is located in Bao'an District in western Shenzhen. Fig. 1 shows the location map of this case study. The tunnel project between Chentian Station and Northern Chentian Station of Shenzhen Metro Line 12 (abbreviation: Chen-Chen section) is designed as a single tunnel with two lines. The length of the whole line is 1040.826 m, the burial depth of the tunnel is approximately 11~23 m. The section tunnel passes through moderately weathered, weakly weathered and slightly weathered leptynite strata, respectively. Fig. 2 presents the petrographic characteristics of leptynite under a microscope. The leptynite is grayish white and the main mineral components are alkaline feldspar (49%, 0.50-8.06 mm), plagioclase (20%, 0.30-3.70 mm), quartz (25%, 0.20-6.15 mm), biotite (5%, 0.10-2.13 mm), and metallic minerals (1%, 0.05-0.68 mm), and it has a medium to coarse semi-automorphic granular crystal structure or residual sandy structure and massive structure. Fig. 3 shows the geological section of the metro tunnel. Because of the relatively long interval of hard leptynite and the variability

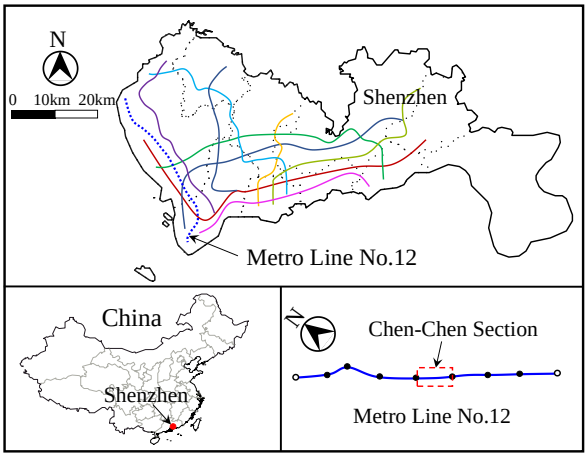

Fig. 1 The location map of Shenzhen Metro Line No. 12 (Chen-Chen section)

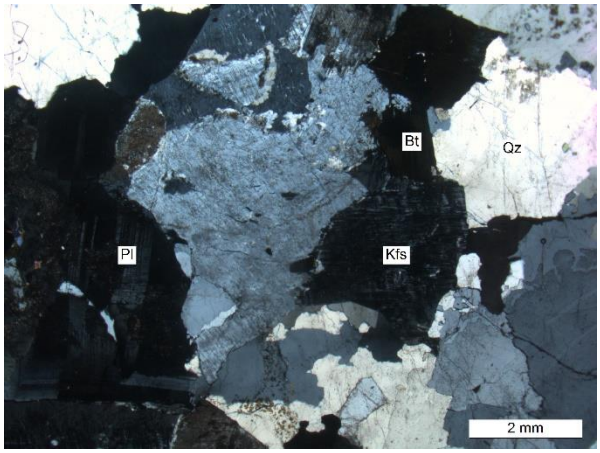

Fig. 2 The petrographic characteristics of leptynite under a microscope

Table 1 Summary of the main rock characteristics in this study.

No.	Initiate tunneling mileage	Interval length (m)	Rock type	Rock morphology	*Kv*	Rock mass classification	*UCS* (MPa)	
							Avg	Range
Z1	ZCK18+793.42	34.33	Leptynite	Partial block	0.18	V	43.7	20.7-58.5
Z2	ZCK18+827.75	77.75	Leptynite	–	0.61	III	103.8	89.6-118.7
Z3	ZCK18+905.50	311.45	Leptynite	–	0.53	III、IV	148.5	123.2-157.3
Z4	ZCK19+216.95	79.47	Leptynite	–	0.56	III	173.7	163.8-184.5
Z5	ZCK19+296.42	89.57	Leptynite	Partial block	0.52	III、IV	118.6	97.8-134.1
Z6	ZCK19+385.99	13.35	Leptynite	Massive blocks	0.20	V	60.5	48.7-68.6
Y7	YCK18+753.21	81.75	Leptynite	Partial block	0.34	IV、V	77.8	56.3-84.2
Y8	YCK18+834.96	138.59	Leptynite	–	0.45	III	108.3	88.7-113.4
Y9	YCK18+973.55	108.51	Leptynite	–	0.53	III	130.7	121.7-139.7
Y10	YCK19+082.06	129.45	Leptynite	–	0.57	III	100.3	93.4-107.6
Y11	YCK19+211.51	236.8	Leptynite	Partial block	0.38	III、IV、V	79.4	54.3-88.7
Y12	YCK19+522.21	21.86	Leptynite	Massive blocks	0.22	V	58.7	37.8-65.4

of geological parameters along the project, the preliminary investigation of engineering geological information is carried out by drilling multiple exploration holes before the project excavation to obtain as accurate geological characteristics as possible. Thus, as shown in Fig. 3, the study area was divided into a total of 12 excavation intervals using 15 geological exploration holes, including 6 each in the left and right lines. Fig. 4 depicts the core properties of some boreholes in the field. First, the uniaxial compressive strength (UCS) of the rock samples collected

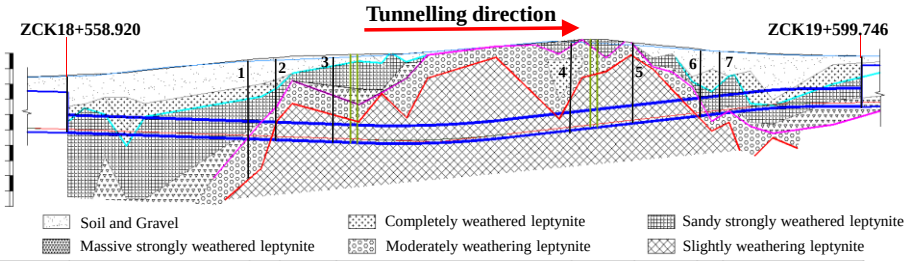

Zone No.	–	Z1	Z2	Z3	Z4	Z5	Z6	–
Geological type	–	Rock						–
Rock mass classification	–	V	III	III, IV	III	III, IV	V	–
Zone distance (m)	–	33.4	77.75	311.45	79.47	89.57	13.35	–

(a) Left line

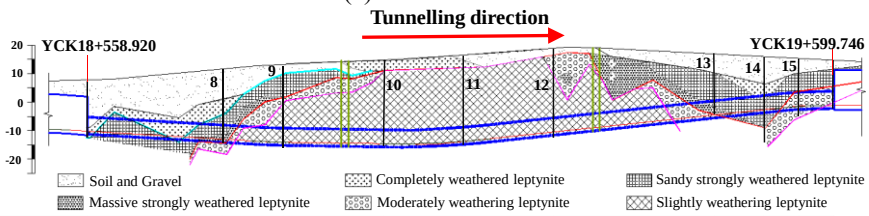

Zone No.	–	Y7	Y8	Y9	Y10	Y11	–	Y12	–
Geological type	–	Rock					–	Rock	–
Rock mass classification	–	IV, V	III	III	III	III, IV, V	–	V	–
Zone distance (m)	–	81.75	138.59	108.51	129.45	236.8	–	21.86	–

(b) Right line

Fig. 3 Geological profile of the Chen-Chen excavation section. (a) Left line and (b) right line

Fig. 4 The core properties of some boreholes in the field

using the geological exploration holes were tested according to the method recommended by ISRM (1979), and the approximate value of *UCS* for each excavation interval was estimated by calculating the average value of *UCS* of two adjacent exploration holes. In addition, acoustic tests were performed on all exploration holes to obtain the intactness index of the rock mass (K_V) with reference to the Standard for Engineering Classification of Rock Masses (The National Standards Compilation Group of People's Republic of China, GB/T 50218–2014). K_V is defined as the square of the ratio of the *p*-wave velocity of the rock mass (V_{pm}) (m/s) to the *p*-wave velocity of the intact rock (V_{pi}) (m/s), i.e., $K_V = (V_{pm}/V_{pi})^2$, which can describe the fracture degree and discontinuity conditions of the rock mass.

Subsequently, the quartz content of the leptynite section was also investigated and was at a high level overall,

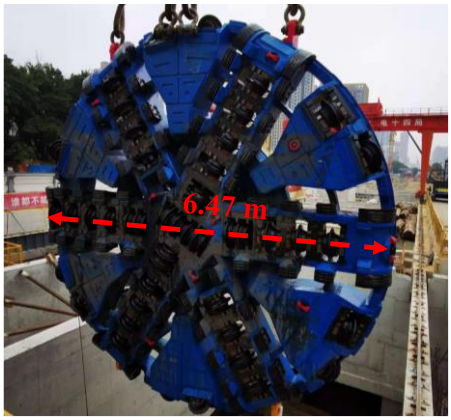

(a) Cutterhead

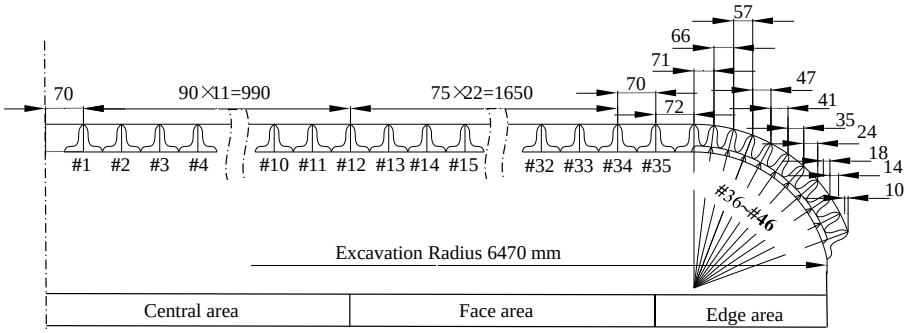

(b) Schematic diagram of TBM cutterhead

Fig. 5 Actual cutterhead object and schematic diagram of the TBM cutterhead. (a) Cutterhead and (b) schematic diagram of the TBM cutterhead

Table 2 Main specifications of the TBM in this study

Technical parameter	Description
TBM model	Dual-mode
Machine diameter (m)	6.47
Number of cutters	47
Disc nominal spacing (mm)	75
Power of whole machine (kW)	1668.05
Cutterhead nominal torque (kN·m)	6228
Max. thrust cutterhead (tons)	4225
Cutterhead RPM (r/min)	0-4.4
Cutterhead advance speed (mm/min)	0-80
Cutter diameter (mm)	457
Cutter tip width (mm)	19
Max. thrust per cutter (kN)	250
TBM weight (tons)	Approx. 500

ranging from 35% to 40%. Finally, the rock mass was classified according to the Standard for Engineering Classification of Rock Masses (The National Standards Compilation Group of People's Republic of China, GB/T 50218–2014) between III and V. Table 1 presents the distribution and geological data of 12 excavation intervals.

As shown in Fig. 3 and Table 1, the tunnel mainly passes through the slightly weathered leptynite stratum with high rock strength. The uniaxial compressive strength of the rock ranges from 20.7 to 184.5 MPa. There are five intervals with *UCS* < 80 MPa, including the Z1, Z6, Y7, Y11 and Y12 intervals; there are four intervals with 80 MPa < *UCS* < 120 MPa, including the Z2, Z5, Y8 and Y10 intervals; there are two intervals with 120 MPa < *UCS* < 160 MPa, which are Z3 and Y9; and only the Z4 interval exhibits *UCS* > 160 MPa. The rock mass of the whole project has good integrity, and the rock types are mostly classes III, IV and V. The total length of the hard rock section is 1326 m, of which the left line section is approximately 608 m and the right line section is approximately 718 m, accounting for 58% and 69% of the section excavation length, respectively. The content of quartz is between 30% and 40%. Therefore, due to the complex long-distance hard leptynite geological conditions, the sharp consumption of cutters during TBM tunneling seriously restricts the construction progress and increases the additional cost.

2.2 TBM specification

This project adopts two dual-mode TBMs from Herrenknecht with an excavation diameter of 6470 mm. Fig. 5 shows the actual cutterhead object and a schematic diagram of the TBM cutterhead. The main specifications of the TBM in this study are listed in Table 2. As shown, it can be concluded that there are 47 18-in disc cutters in the whole cutterhead (a double-ring cutter is regarded as a two-disk cutter when numbering). The cutter positions of #1~#12 are the center double-ring disc cutters with a cutter space of 90 mm, located in the central area; the #13~# 35

Table 3 Statistical description of disc cutter consumption in this study (piece)

Cutter type	Failure form of cutter					Total replacements
	Uniform wear of the cutter ring	Flat wear of the cutter ring	Curling of the cutter blade	Cracking and spalling of the cutter ring	Other abnormal wear	
Center cutter	68	12	4	10	9	103
Face cutter	244	22	7	10	8	291
Gage cutter	250	36	6	6	6	304
Total replacements	562	70	17	26	23	698

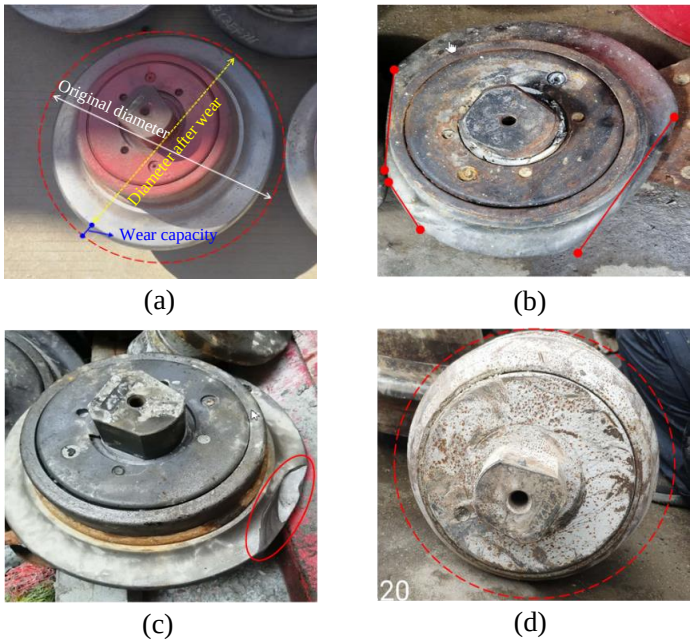

Fig. 6 Wear types of the disc cutters. (a) Uniform wear of the cutter ring, (b) flat wear of the cutter ring, (c) cracking of the cutter ring and (d) spalling of the cutter ring

cutter positions are the face disc cutters with a cutter space of 75~70 mm, located in the face area; and the # 36~# 46 cutter positions are the gage disc cutters with a cutter space of 72~10 mm, located in the edge area. In particular, the #46 cutter position is installed with two identical disc cutters, also called copy cutters. The material hardness of the cutter ring is 50~60 HRC.

3. Failure statistics and wear analysis of disc cutter

3.1 Statistics of failure forms of disc cutter

Owing to the high strength and high abrasiveness of the hard leptynite zone, the problems of cutter wear and replacement frequency are very prominent. Consequently, a large wear database was developed. The wear and replacement of 698 disc cutters are obtained by tracking the field data of 1326 m excavation mileage. Table 3 lists the statistical overview of the disc cutter consumption. It can be determined that the failure types of disc cutters are mainly divided into normal wear and abnormal wear. As shown in Fig. 6(a), normal wear refers to the gradually uniform wear of the whole cutter ring with the increase of excavation mileage, and the blade becomes wider to a certain extent, resulting in the decline of the rock-breaking ability or failure to cut rock, which is also called uniform wear. In Figs. 6(b)-6(d), abnormal wear mainly includes flat wear (chord wear), cracking, or spalling of the cutter ring. Flat wear, also called nonuniform wear, is a phenomenon mainly caused by serious local wear of the cutter ring when the rotation of the disc cutter occurs unsteadily or even stops, thus triggering part of the cutter ring wear as a flat surface. In particular, in this project, curling of the cutter blade, bearing fracture and bolt loosening, and other failure forms also occurred. The overworn cutter rings and other failed components were changed during the daily inspection. It was found that 562 disc cutters were replaced due to normal wear, accounting for approximately 81% of the total. Abnormal damage led to 136 disc cutter replacements, accounting for approximately 19% of the total.

The total number of disc cutters replaced due to normal wear at each mounting position is illustrated in Fig. 7. Since the disc cutters in different installation areas have special cutting tasks, the allowable wear depth of the cutter ring is set at different values. To ensure excellent rock-cutting

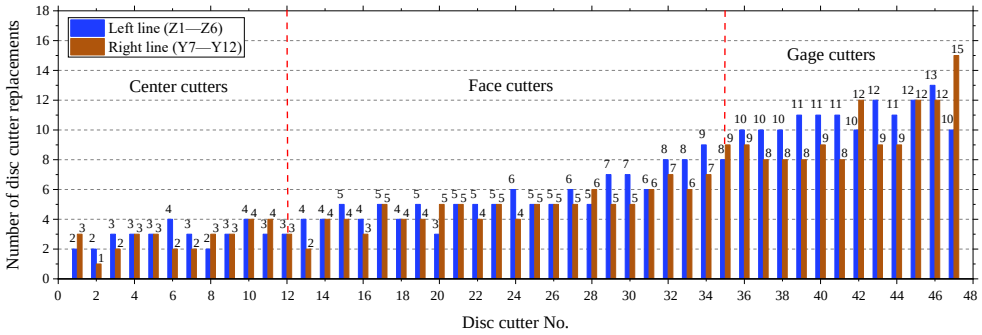

Fig. 7 Consumption of the disc cutter caused by normal wear for each position

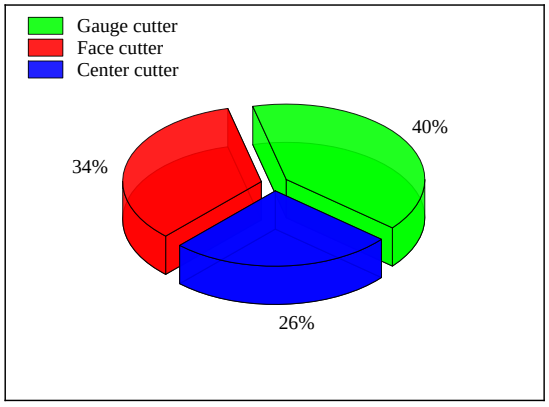

Fig. 8 Consumption of abnormal wear in different areas of the cutterhead

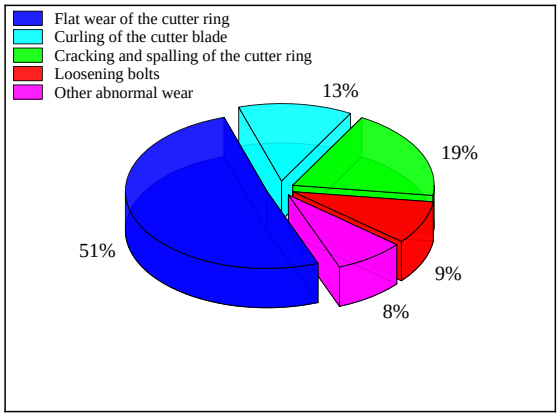

Fig. 9 Consumption of each abnormal wear type of the disc cutter

efficiency of the cutterhead, the central area and the face area are set at 15 mm and 20 mm, respectively, so the replacement frequency is low. The edge area is set at 10 mm (the #46 disc cutter is 5 mm) to ensure adequate tunneling clearance and prevent the TBM from getting stuck or becoming difficult in the turning direction, leading to more frequent replacement. The consumption rate of disc cutter is closely related to the cutter position number or installation radius. The general trend is that the consumption rate increases with the increase of the disc cutter position number. As explained by Wang *et al*. (2015), the reason is that the linear speed of each disc cutter and the total length of the cutting path increase with the increase of its installation radius, so cutter wear will be accelerated. As shown in Fig. 8, the abnormal wear rate of disc cutters in the edge area is the highest (54 pieces, 40%), which is mainly because the gage cutters were often required to bear the secondary rock-breaking action. They are specifically characterized by cutter ring cracking and bearing breakage at a higher speed, as well as violent collision failure during starting and braking at higher acceleration. The second highest is the face area of the cutter (47 pieces, 34%), which experienced a higher number of cutter ring dislodgements. The wear rate of the central area is relatively low (35 pieces, 26%), and flat wear is prone due to the lower linear velocity of the center cutter and its higher rotational resistance and eccentric load. In addition, the proportional distribution of abnormal wear is shown in Fig. 9. It is obvious that flat wear is the main type of abnormal damage, accounting for approximately 51% of the abnormal damage. Approximately 19% and 13% of the total damage was caused by the cracking or spalling of the cutter ring and blade curling, respectively. Therefore, it is necessary to check whether the cutter ring has oil leakage and cracks before using the cutter and then adopt special tools to test the cutter to check the starting torque. Furthermore, the starting torque in the tunneling process should be adjusted according to the surrounding rock conditions.

3.2 Analysis of the disc cutter wear rate

Since uniform wear is the main reason for disc cutter consumption, it is necessary to evaluate and predict disc cutter consumption caused by uniform wear, which can provide necessary basis for making a reliable cutter change plan and estimating an accurate cutter consumption cost. In the course of a large number of previous analyses and studies, engineers usually use the wear rate to evaluate the general trend of on-site cutter uniform wear according to the section shape characteristics of the disc cutter ring, which has achieved a good application effect (Ewendt 1989, Wan *et al*. 2002a, b, Zhao *et al*. 2014, Sun *et al*. 2019, Lan *et al*. 2020). However, most of the analyzed objects only involve single-blade or double-blade disc cutters, as well as face-area disc cutters, without a comprehensive investigation of each disc cutter located in the whole cutterhead. Therefore, by tracking and statistically analyzing the wear capacity of disc cutters in the field, this paper adopts the radial wear rate to evaluate the wear law of

the whole cutterhead area, which is defined as the total radial wear capacity of the disc cutter under the unit tunneling distance of the TBM. The radial wear rate can be expressed as

$$WR(i)=\frac{M_i}{L},\ \ i=1,\cdots,n \tag{1}$$

where $WR(i)$ represents the radial wear rate of the disc cutter on the i^{th} installation position, mm/m; M_i represents the accumulated radial wear capacity of the disc cutter on the i^{th} installation position; and L represents the cumulative tunneling distance of the TBM.

By analyzing and compiling the accumulated normal wear of the disc cutters at each position tracked and measured in the field, a large database of disc cutter wear is established. The accumulated wear of the disc cutters will be recalculated when the TBM enters a different excavation interval. On this basis, the radial wear rate curves of the disc cutter at each position in 12 excavation intervals are obtained, as shown in Fig. 10. The broken line denotes the actual wear rate of the disc cutters, and the straight line denotes the fitted wear rate. The analysis results suggest that the wear rate of disc cutters has a roughly linear relationship with the installation radius of the cutter, and the consumption and installation radius of disc cutters in this project also reflect this law. In addition, since there is no disc cutter arrangement when R_i = 0, $WR(i)$ is also equal to 0, i.e., the curve has no Y-intercept. Thus, it is reasonable and reliable to use a directly proportional function for fitting in this paper.

Fig. 10 shows that the actual wear rate of the disc cutter fluctuates within a certain range, performing different fluctuation rules with the installation radius. In the face area and central area, the actual wear rate is close to the fitting value. In the edge area, it is higher than the fitting value, which is consistent with the conclusion of the disc cutter consumption law. In addition, the fluctuation law has a large variability within different excavation geological intervals. In Figs. 10(a), 10(f), 10(g), 10(k), and 10(l), the position indicated by the red circle represents the abnormal uniform wear of the disc cutters with a sharp increase in the wear rate, which is probably due to the TBM tunneling the rock fracture layer and the disc cutters repeatedly acting on raised hard particles or large pieces of rocks, accelerating the plastic removal process of the cutter rings and leading to intense uniform wear. In contrast, the position shown by the green circle represents that the disc cutters are not rock-cutting sufficiently, and the disc cutters tend to become idle, so the wear rate is lower than the normal value. It is worth noting that, except for Y11, the total lengths of the other excavation intervals mentioned above are relatively short (13.35~81.75 m). When the rock *UCS* is relatively low, the cutter wear rate is relatively small. If the disc cutter exhibits abnormal uniform wear, there will be large fluctuations. In particular, Z6 (13.35 m) in Fig. 10(f) leads to an R^2 value of only 0.618. In Fig. 10(k), although the rock *UCS* in Y11 is also relatively low, the wear rate is relatively high. This is attributed to the rock types in mixed intervals of classes III, IV, and V.

During the rock-breaking process, the disc cutter is vulnerable to material removal resulting in wear because of the great impact force caused by the alternation of soft rock and hard rock. Moreover, the falling and secondary wear of large rocks undoubtedly increase the drastic wear of disc cutters. Although this excavation interval is relatively long (236.8 m), the cutter wear rate fluctuates greatly, resulting in an R^2 value of 0.609. As shown in Table 1 and Figs. 10(b), 10(c), 10(d), 10(e), 10(h), and 10(j), the cutter wear rate exhibits a significant increasing trend as the overall rock *UCS* increases. The abnormal uniform wear of the disc cutters tends to occur in the rock fracture zone, and its probability of occurrence decreases significantly with increasing K_V, resulting in a decrease in the overall fluctuation of the curve. The R^2 values are all greater than 0.8, and the highest is 0.854. In general, if only the installation radius is considered, the direct proportion function can better reflect the wear characteristics of each disc cutter. Therefore, Eq. (2) can be obtained as follows

$$WR(i)=KR_i \tag{2}$$

where $WR(i)$ represents the radial wear rate of the disc cutter on the i^{th} installation position, mm/m; K represents the slope coefficient of the direct proportion fitting function, mm/m·mm; and R_i represents the installation radius of the i^{th} disc cutter position, mm.

Based on Eq. (2), when the parameters reflecting the geological characteristics and TBM tunneling performance are maintained at a constant value in a certain interval, it can be concluded that the wear rate of the disc cutter is only related to the installation radius. However, due to the complexity and variability in geological information and tunneling parameters, it is obviously unreasonable to use only a constant value to evaluate the cutter wear of long-distance tunneling. It has been reported that the disc cutter wear law will show significant differences with changes in geological characteristics and tunneling parameters (Liu *et al.* 2017, Su *et al.* 2020). Therefore, to quantitatively analyze the correlation between the cutter wear rate and geological characteristics and TBM performance, Table 4 lists the average values of the TBM performance parameters and wear rates in 12 excavation intervals, and the average value is selected to denote the general trend of the wear law in a single interval. The FPI in Table 4, i.e., the field penetration index (kN/cutter/mm/rev), is a new TBM tunneling performance evaluation index (Gong *et al*. 2009, Hassanpour *et al.* 2010, 2011). The *FPI* is composed of two important parameters F_n (disc cutter load or normal force) and p (penetration per revolution of the cutterhead). It is defined as follows

$$FPI=\frac{F_n}{p} \tag{3}$$

where F_n represents the load or normal force acting on each disc cutter, i.e., $F_n = (TF\text{-}f)/n$, kN/cutter; TF represents the total thrust of the TBM cutterhead during normal tunneling, kN; and f represents the total friction force when TF is applied, kN. Delisioet et al. (2014) suggested that f should be approximately 20% of the TBM weight; n represents the total number of disc cutters installed on the TBM cutterhead; and p represents the penetration per revolution

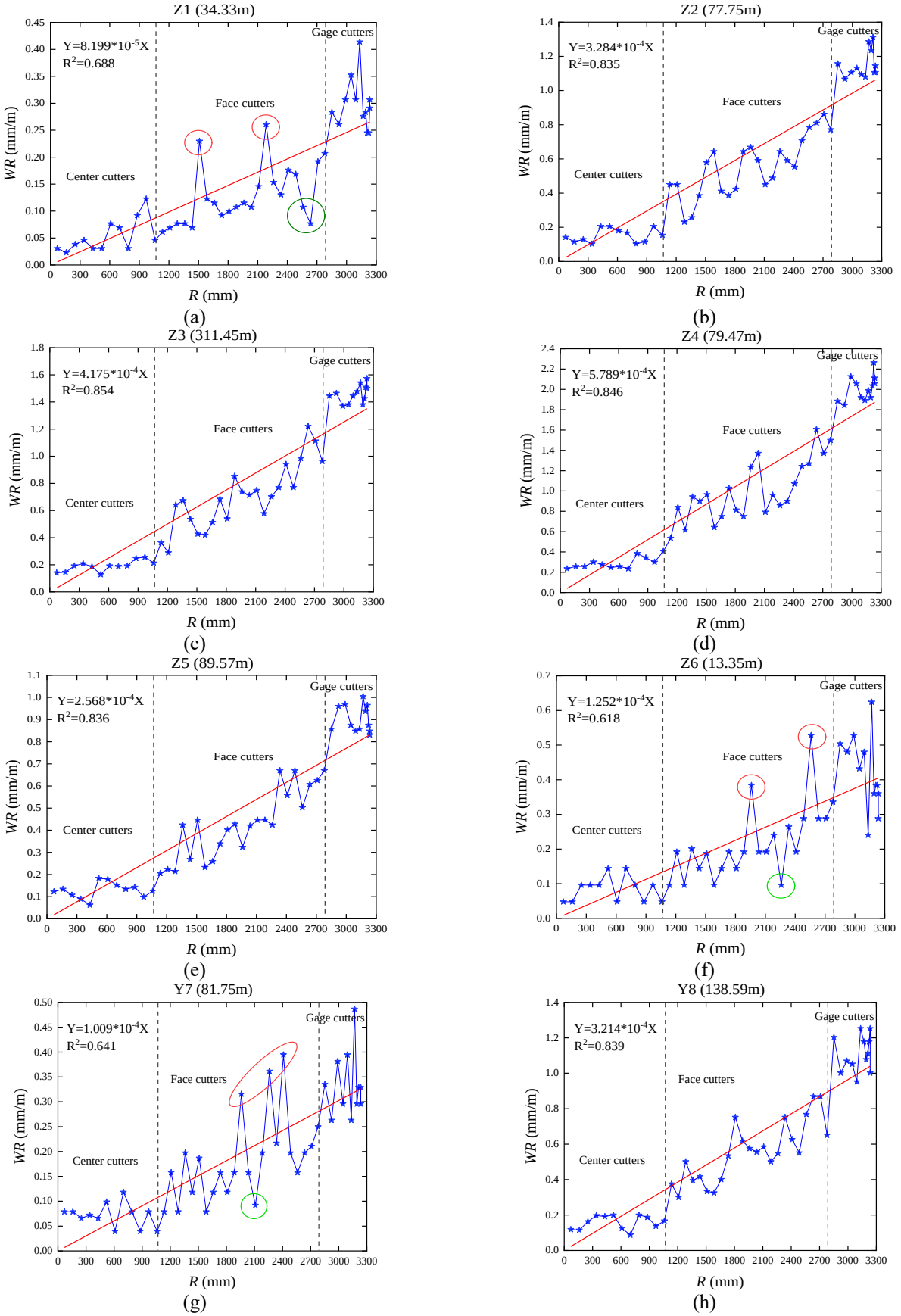

Fig. 10 Disc cutter wear rate of different advance sections. (a) Z1, (b) Z2, (c) Z3, (d) Z4, (e) Z5, (f) Z6, (g) Y7, (h) Y8, (i) Y9, (g) Y10, (k) Y11 and (l) Y12

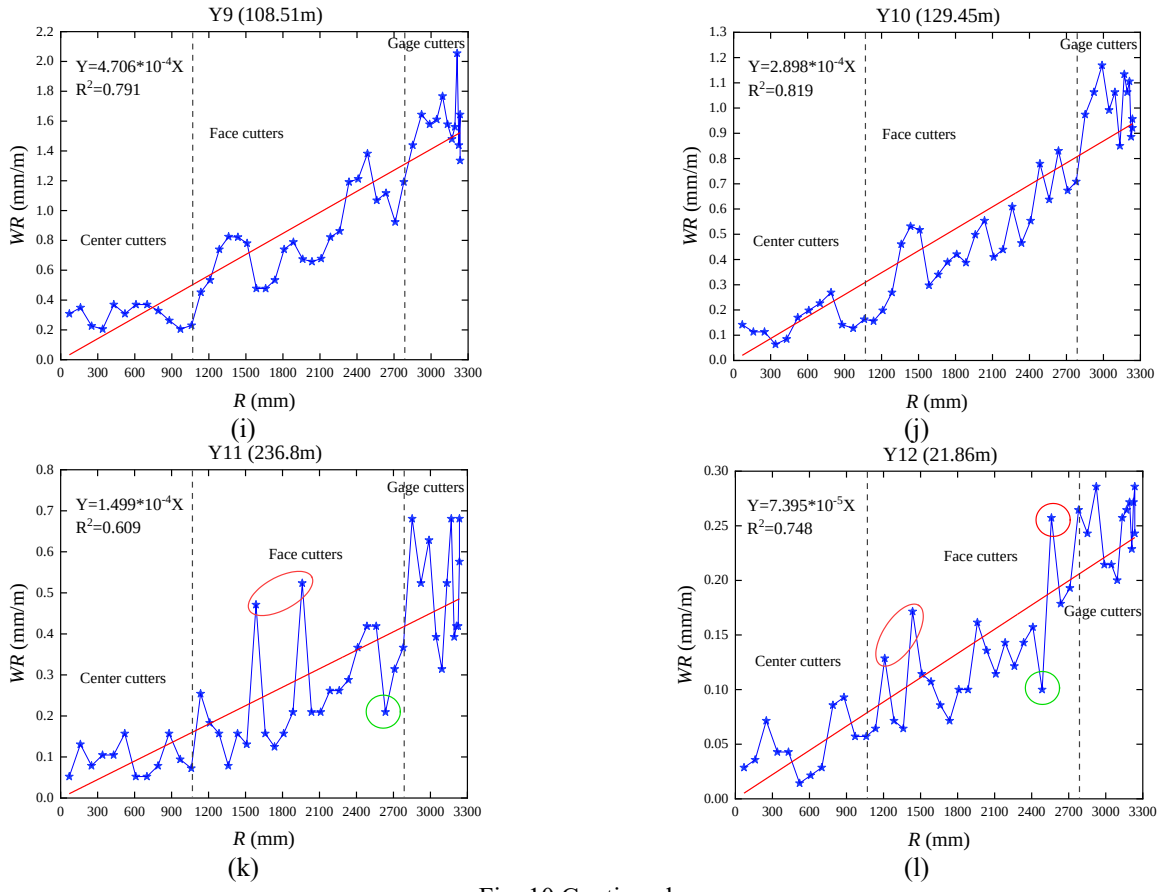

Fig. 10 Continued-

of the cutterhead, mm/rev. The *FPI* can be calculated by simply testing or estimating these two parameters.

By analyzing the results in Table 4, it can be concluded that the slope coefficient K of the linear fitting function between the wear rate of disc cutters and the installation radius ranges from 7.395×10^{-5} to 5.789×10^{-4} mm/m·mm in leptynite, and the maximum value (Z4) is similarly 8 times the minimum value (Y12). Fig. 11 shows the linear fitting function curve of the wear rate in 12 intervals. Fig. 11 shows that the geological parameters (e.g., *UCS* and K_V) and TBM performance parameters (e.g., p and *FPI*) of each excavation interval are closely related to the wear rate *WR*.

- The first type is the case of slightly hard rock. For the Z1, Z6, Y7, Y11, and Y12 intervals, as shown in Fig. 11, the *UCS* is less than 80 MPa, and K_V is between 0.18 and 0.38. When the average penetration is 10.15, 12.64, 8.86, 10.26, and 15.33 mm, the *FPI* is less than 18 kN/cutter/mm/rev. The results imply that for the #1~#47 disc cutters installed on the cutterhead, when the overall average wear rate of the cutterhead is less than 0.30 mm/m, the slope coefficient of the fitting function is less than 1.5×10^{-4} mm/m·mm, which indicates slight abrasion.
- The second type is the case of moderately hard rock. For the Z2, Z5, Y8, and Y10 intervals, as shown in Fig. 11, the *UCS* ranges from 80 to 120 MPa, and K_V ranges from 0.45 to 0.61. When the average penetration is 7.66, 9.64, 8.01, and 6.69 mm, the FPI is between 14 and 33 kN/cutter/mm/rev. The results indicate that for the #1~#47 disc cutters installed on the cutterhead, when the overall average wear rate of the cutterhead is between 0.48 and 0.63 mm/m, the slope coefficient of the fitting function ranges from 1.5×10^{-4} to 2.5×10^{-4} mm/m·mm, which indicates moderate abrasion.
- The third type is the case of very hard rock. As shown in Fig. 11, for the Z3 and Y9 intervals, the *UCS* ranges from 120 to 160 MPa, and K_V is 0.53. When the average penetration is 6.67 and 5.88 mm, the *FPI* is between 35 and 40 kN/cutter/mm/rev. The results show that for the #1~#47 disc cutters installed on the cutterhead, when the overall average wear rate of the cutterhead is between 0.79 and 0.90 mm/m, the slope coefficient of the fitting function ranges from 2.5×10^{-4} to 4.5×10^{-4} mm/m·mm, which indicates high abrasion.
- The fourth type is the case of extremely hard rock. For the Z4 interval, as shown in Fig. 11, the *UCS* exceeds 160 MPa, and K_V is greater than 0.56. When the average penetration is 6.97 mm, the *FPI* is 35 kN/cutter/mm/rev. The results suggest that for the #1~#47 disc cutters installed on the cutterhead, when the overall average wear rate of the cutterhead is 1.10 mm/m, the slope coefficient of the fitting function is approximately 5.8×10^{-4} mm/m·mm, which indicates extreme abrasion.

Table 4 The average values of TBM performance parameters and wear rates in 12 excavation intervals

No.	F_n (kN/cutter)	p (mm/rev)	FPI (kN/mm/rev)	This work	
				K (10^{-4}mm/m·mm)	R^2
Z1	163.06	10.15	16.06	0.820	0.688
Z2	192.25	7.66	25.10	3.284	0.835
Z3	237.08	6.67	35.54	4.175	0.854
Z4	244.37	6.97	35.06	5.789	0.846
Z5	140.12	9.64	14.54	2.568	0.836
Z6	164.52	12.64	13.02	1.252	0.618
Y7	149.92	8.86	16.92	1.009	0.641
Y8	180.36	8.01	22.52	3.214	0.839
Y9	229.99	5.88	39.11	4.706	0.791
Y10	216.23	6.69	32.32	2.898	0.819
Y11	179.11	10.26	17.46	1.499	0.609
Y12	128.86	15.33	8.41	0.740	0.748

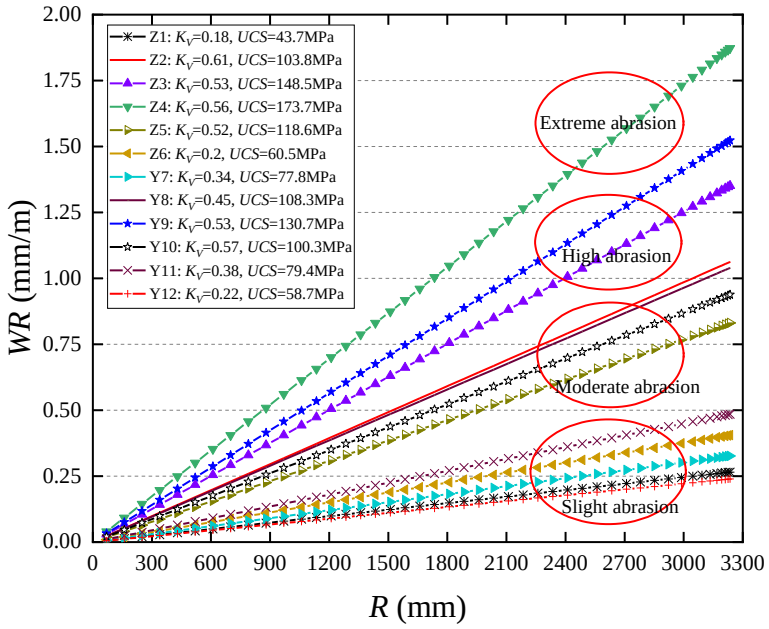

Fig. 11 Curve of linear fitting function of disc cutter wear rate of 12 intervals

4. Prediction model for the wear rate of the disc cutter

4.1 Parameter selection

Based on the abovementioned statistics and analysis results of disc wear, the main factors affecting the wear capacity of the disc cutter include the cutterhead structure and cutter layout (e.g., cutter spacing, edge transition curve, gage cutter height difference, etc.), disc cutter characteristic parameters (e.g., cutter size, blade width and shape, material and hardness of the cutter ring, etc.), and abnormal damage (e.g., flat wear, cutter ring cracking or spalling, bearing fracture, bolt loosening, etc.). Additionally, a large number of field tests show that cutter wear is also closely related to geological characteristics (e.g., *UCS*, *RQD*, K_V, joint, quartz content, etc.) and TBM tunneling performance (e.g., *p*, *RPM*, *TF*, *FPI*, etc.) (Liu *et al.* 2017, Sun *et al.* 2019, Li *et al*. 2020, Su *et al.* 2020, Shen *et al*. 2022). It is noteworthy that the statistical process of disc cutter wear is often quite different due to the influence of many complex factors. In fact, it is impossible to consider all cases and exclude all anomalies (Yan *et al.* 2019, Lan *et al.* 2020). However, by comparing and analyzing real data in the field, the selection of representative and reliable parameters or indicators can predict the overall trend of disc cutter wear, which is of great significance for engineers to understand the wear performance of disc cutters.

The laboratory wear test results of disc cutters show that the main reason for uniform wear is plastic removal abrasiveness, which accounts for approximately 82.9% of the total wear (Zhao *et al.* 2014). Generally, microcutting and microfurrowing will lead to a uniform wear rate of materials by abrasive degradation, i.e., abrasive particles press into the material and move relative to the surface to

Table 5 Summary results of the determination of the regression coefficients of correlation between different parameters and *WR*

Parameters	Regression coef. (R^2)	Regression type	Relationship	Equation No.
K_V	0.802	Exponent	$WR(i)=3.815\times10^{-5}e^{4.086K_V}R_i$	(4)
UCS (MPa)	0.905	Linear	$WR(i)=(4.067\times10^{-6}UCS-1.418\times10^{-4})R_i$	(5)
F_n (kN)	0.686	Exponent	$WR(i)=1.302\times10^{-5}e^{0.015F_n}R_i$	(6)
p (mm/rev)	0.715	Power	$WR(i)=0.021p^{-2.117}R_i$	(7)
FPI (kN/cutter/mm/rev)	0.783	Linear	$WR(i)=(1.431\times10^{-5}FPI-6.286\times10^{-5})R_i$	(8)

form a furrow. Finally, the material is removed by forming chips (Liu *et al.* 2017, Sun *et al.* 2019). According to the particle abrasiveness model of the microcutting hypothesis proposed by Rabinowicz (1995), the wear capacity of the material is directly proportional to the normal force and sliding distance and inversely proportional to the yield strength of the material σ_s or hardness of the material *H*. Considering the geometric movement of the disc cutter, the trajectory of the rock-breaking point is closely related to the size, installation position and advancing speed or penetration of the disc cutter (Sun *et al.* 2019). That is, when the characteristic parameters of the cutter are constant, the normal force F_n acting on the disc cutter and the penetration p of the cutterhead directly determine the wear capacity of the cutter ring. Meanwhile, the Colorado School of Mines (CSM) model emphasizes that F_n and *UCS* are the main determining factors of p. The analysis results show that p decreases as the rock *UCS* increases under the same cutterhead thrust conditions (Rostami 1997). In fact, geological characteristics usually indirectly affect disc cutter wear by influencing TBM tunneling performance. Hassanpur *et al*. (2010, 2011) suggested a strong correlation between geological parameters (e.g., *UCS* and *RQD*) and *FPI*. In addition, Lan *et al*. (2020) concluded that the influence of quartz content and joints can be disregarded when the only rock type in the study area is leptynite, with an average quartz content of 35~40% and no obvious fracture zones. Based on this context, this paper only investigates the influence of *UCS*, K_V, p, F_n and *FPI* on the wear capacity and establishes the correlation between them and the slope coefficient (*K*) in Eq. (2) and proposes the most suitable evaluation model of the disc cutter wear rate. When *K* is determined, the prediction model of the disc cutter wear capacity relevant to researchers, i.e., Eq. (1), will also be obtained.

4.2 Development of the prediction model

In underground engineering practice, empirical equations based on mathematical statistics have been extensively used to predict the target performance index based on geological or other operational parameters. Compared with extensive theoretical analysis, empirical equations have higher importance during the early stages of engineering design since they are more practical and come from actual projects (Zhang *et al.* 2015, Zhou *et al.* 2016, Sun *et al.* 2022). In this study, the regression analysis method is used to derive the relationship between the wear rate of disc cutters and the engineering geological parameters and TBM performance parameters. The cutter wear rate estimation model is established by simple regression and multivariable regression analyses.

To develop simple empirical equations for the disc cutter wear rate under similar geological conditions, the relationships between the slope coefficient *K* in Eq. (3) and *UCS*, K_V, p, F_n, and *FPI* were evaluated by using simple bivariate regression analysis. The correlation results of *K* with different geological and performance parameters are shown in Fig. 12 and Table 5.

From Fig. 12, it can be concluded that *K* presents several different function growth trends with increasing K_V, *UCS*, F_n, and *FPI*. Conversely, *K* remains negatively correlated with p in the form of a power function. In other words, the correlation with p is the opposite those with K_V, *UCS*, F_n, and *FPI*. Simultaneously, in Fig. 12(d), it can be inferred that when the cutterhead thrust increases to a certain value, the thrust will not continue to increase due to the limitation of the extreme maximum thrust of the disc cutter (i.e., 250 kN). In addition, according to the results in Table 5, the selected geological and performance parameters show a good correlation with the slope coefficient even as a single input variable (R^2=0.686~0.905). The correlation between geological parameters and the cutter wear rate is better compared with the performance parameters, especially *UCS* (R^2=0.905), which implies that *UCS* is the most dependent parameter to explain the wear rate. Similarly, for the performance parameters, *FPI* also shows a good correlation (R^2=0.783), mainly because it combines the two characteristics of p and F_n. When the equipment maintains a certain thrust, the increase in *FPI* indicates that the rock hardness strengthens and it is more difficult to penetrate the rock. This means that the turning times of the cutterhead per unit tunneling distance will increase, and the rock-breaking path will also expand, resulting in the aggravation of disc cutter wear.

In addition to simple regression analysis, the multiple regression method is also used to find an empirical equation with the best fit to existing data. A total of five parameters, K_V, *UCS*, F_n, and *FPI*, are regarded as independent variables, and *K* is regarded as the dependent variable. First Optimization (1stOpt) software was used to carry out the multivariable regression analysis. By considering different

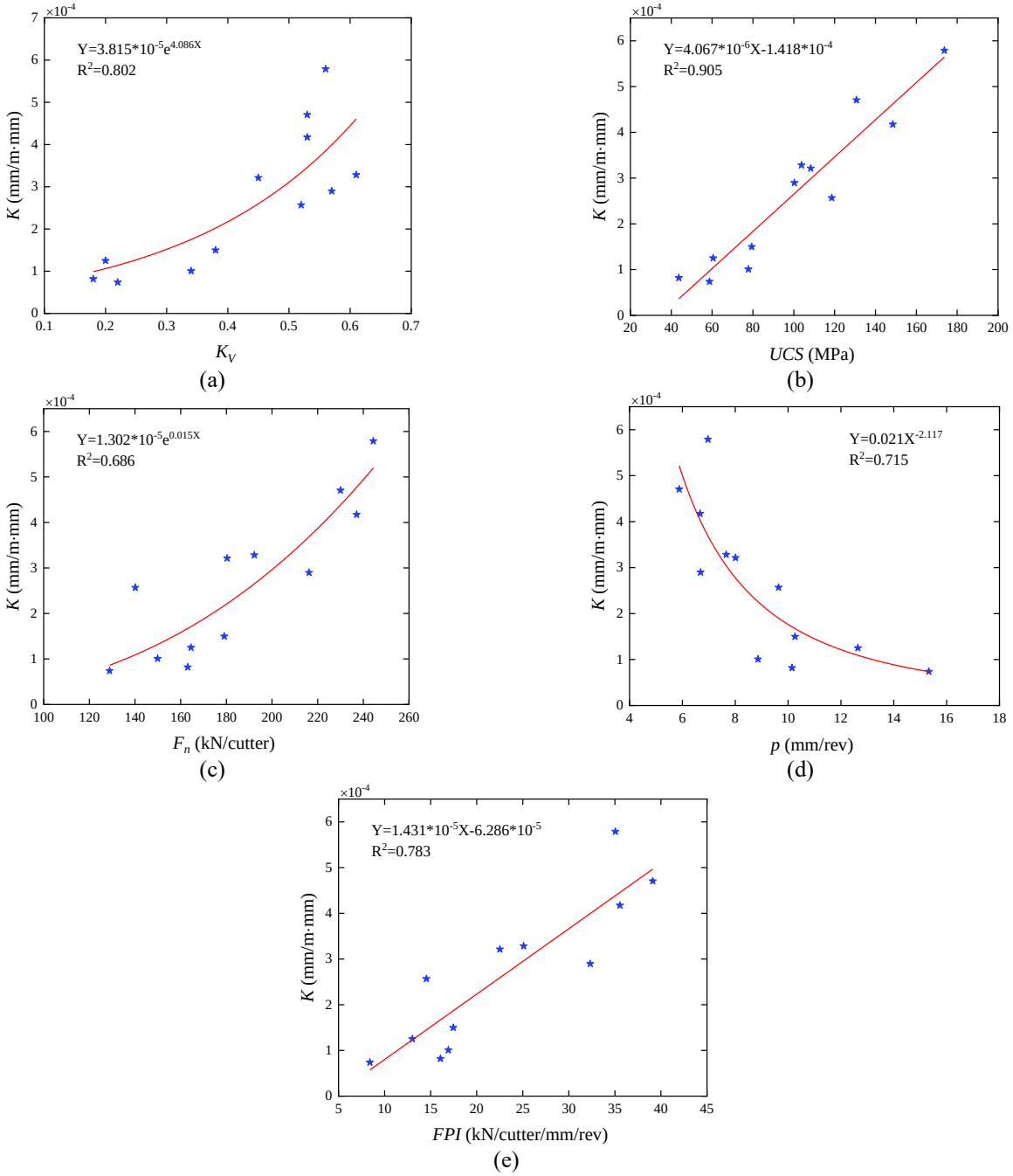

Fig. 12 Relationship between the fitted wear rate (WR) and different parameters. (a) *KV*, (b) *UCS*, (c) F_n, (d) *p* and (e) *FPI*

parameter combinations and developing a series of linear and nonlinear models, the best results that can be identified to predict the disc cutter wear rate index were finally obtained. As a result, a new prediction model is introduced

$$WR(i)=1.018\times10^{-6}e^{0.876K_V}UCS^{1.039}F_n^{0.266}p^{-0.513}R_i \quad (9)$$

where $WR(i)$ represents the radial wear rate of the disc cutter on the i^{th} installation position, mm/m; K_V represents the intactness index of the rock mass; *UCS* represents the uniaxial compressive strength of the rock, MPa; F_n represents the load or normal force acting on each disc cutter, kN/cutter; *p* represents the penetration per revolution of the cutterhead, mm/rev; and R_i represents the installation radius of the i^{th} disc cutter position, mm.

Table 6 presents the summary of the regression model and the ANOVA results. The results show that there is a strong correlation between the dependent variable and independent variables (R=0.978). The independent variables K_V, *UCS*, F_n, and *p* can predict 95.7% of the variance in the dependent variable *WR* (R^2=0.957). The adjusted R^2 indicates that 92.2% of the variable in *WR* around its mean value can be explained by K_V, *UCS*, F_n, and *p*. In addition, *F*-tests related to the utility of the multiple regression model were performed. The results suggest that the correlation is

Table 6 Analysis of variance (ANOVA) for the dependent variable K (confidence level 95%; α = 0.05)

Model summary					
Multiple *R*	0.978				
R square	0.957				
Adjusted *R* square	0.922				
Standard error	4.709e-5				
Analysis of Variance (ANOVA)					
	Sum of squares	Df	Mean square	*F*	Sig.
Regression	2.913e-7	4	7.284e-8	39.59	0.000
Residual	1.291e-8	7	0.184e-8		
Total	1.165e-7	11			

real and the coefficient is true. Therefore, the derived model is statistically significant and effective.

4.3 Evaluation of the prediction model

To evaluate the accuracy of the proposed models, the measured and predicted values of *WR* are compared in Fig. 13. The 1:1 line indicates that the measured *WR* is equal to the predicted *WR*. If the data point is below the 1:1 line, the measured *WR* is greater than the measured *WR*. The results show that most of the predicted values of *WR* are very close to the measured values recorded in the field, with the slope of the fitted line ranging from 0.687 to 0.875 and the R^2 value of the fitted line ranging from 0.719 to 0.891, which can achieve the preliminary prediction of *WR*. Obviously, the slopes of the fitted lines of all models are less than 1.00, indicating a slight overall underestimation of *WR*. In the single variable estimation models, *UCS* presents excellent predictive ability with fitted line slopes and fitted coefficients of 0.844 and 0.867, respectively. By combining some rock mass conditions and tunneling parameters, Eq. (9) exhibits even better predictive power, with the fitted line slope and fitted coefficient improved to 0.875 and 0.891, respectively. To quantitatively evaluate the prediction performance of the six regression models developed in this study, the statistical analysis performance indicators of variance accounted for (VAF) and root mean square error (RMSE) were used for evaluation (She *et al*. 2022a)

$$VAF = \left(1 - \frac{Variance(y_i - \hat{y}_i)}{Variance(\hat{y}_i)}\right) \times 100\% \tag{10}$$

$$RMSE = \sqrt{\frac{1}{N}\sum_{i=1}^{N}(y_i - \hat{y}_i)^2} \tag{11}$$

where y_i represents the measured value, $\hat{y}_i$ represents the predicted value, and N represents the total number of samples. As a whole, the higher the value of VAF is and the lower the value of RMSE is, the better the prediction performance of the model. On the one hand, VAF represents the variability of the predicted value of the model. The value of VAF approaches 100%, meaning that the measured results can be accurately predicted. On the other hand, RMSE explains the deviation in the model, i.e., the offset between the measured values and the predicted values (Li *et al.* 2020, Zhang *et al*. 2021). The VAF and RMSE values corresponding to each model are listed in Table 7.

Table 7 VAF and RMSE calculation results of each prediction model

Prediction models	Performance indices	
	VAF/%	RMSE
Eq. (4)	71.74	0.24
Eq. (5)	86.64	0.17
Eq. (6)	79.96	0.21
Eq. (7)	74.91	0.23
Eq. (8)	79.99	0.21
Eq. (9)	89.06	0.15

The comparison shows that Eq. (9) has the most significant prediction ability, with 89% of the measured values being estimated, which means that Eq. (9) is more statistically reasonable and reliable. Therefore, the developed Eq. (9) can be used to accurately estimate the wear of disc cutters in TBM projects with similar geological characteristics and technical specifications, which is a practical tool for engineers, constructors and contractors.

5. Conclusions

A comprehensive database of disc cutter wear data, geological properties, and tunneling parameters is collected from a recently excavated 1326 m metro tunnel project in leptynite in Shenzhen, China. To acquire more accurate information or parameters, the tunnel is divided into 12 different excavation intervals to study the relationship between the geological characteristics and tunneling parameters with the cutter wear rate in leptynite. The following conclusions are obtained:

- Eighty-one percent of disc cutters are failure due to uniform wear, and other cutters are changed owing to abnormal wear. The center disc cutters have a small rotation radius and thus have a large rotation resistance and eccentric load, which leads to a greater possibility of flat wear. The abnormal wear of the gage disc cutters is mainly because of the high revolution speed

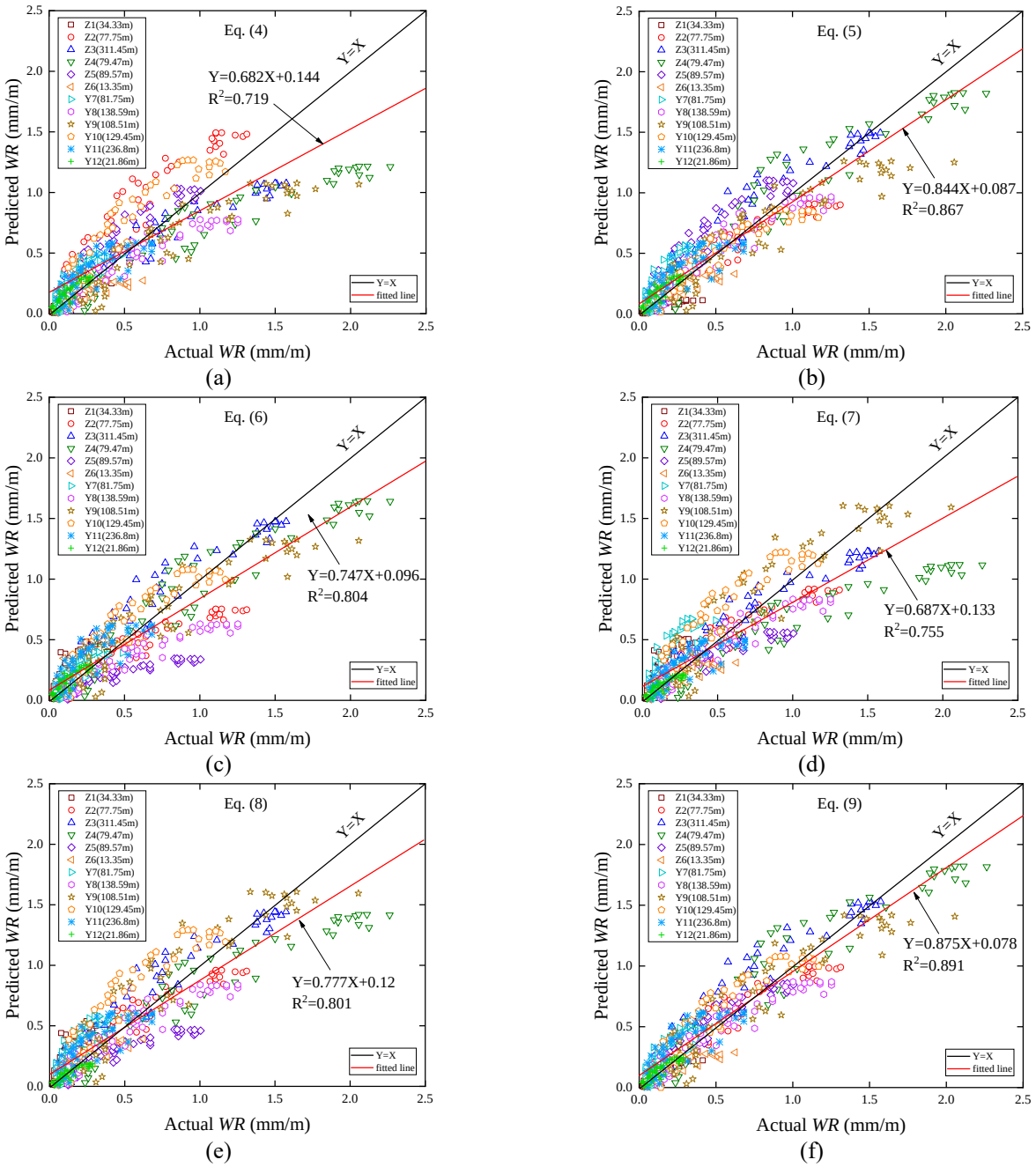

Fig. 13 Comparison of actual and predicted values of the disc cutter wear rate. (a) Eq. (4), (b) Eq. (5), (c) Eq. (6), (d) Eq. (7), (e) Eq. (8) and (f) Eq. (9)

and large impact impulse, resulting in the cutter ring being cracked and the bearing being crushed.

- There is a reasonable direct proportional function relationship between the wear rate of the disc cutter at each position (*WR*) and the installation radius (*R*); thus, an equation for calculating the disc cutter wear rate is established based on the installation radius of the cutterhead. However, due to the variety of geological information and excavation parameters, the fitting slope coefficient (*K*) of the function is also different. A high rock strength tends to result in higher values of *K*.
- Some new empirical equations for predicting the disc cutter wear rate are developed by regression analysis. These equations include five parameters: intactness index of the rock mass (K_V), uniaxial compressive strength of rock (*UCS*), per disc cutter thrust (F_n), penetration (*p*), and field penetration index (*FPI*), which are commonly used parameters easily obtained in the preliminary stages or excavation process of tunnel engineering. The results of the single-factor analysis indicate that the five selected parameters show a good correlation with the wear rate (R^2=0.657~0.870), even if they are all single input variables. One of them, *UCS*, is the most reliable parameter for explaining the *WR*. An estimation model for the disc cutter wear rate based on K_V, *UCS*, F_n, and

p is proposed by using multiple regression analysis, which further improves the accuracy of the prediction model (R^2=0.922). It can predict 89% of the measured *WR* (VAF=89%).

- Since the equations proposed in this study are based on information from individual specific tunnel, it is recommended that they be used only in similar the petrographic characteristics of leptynite, TBM specifications, and operational procedures, not any other rock with different mineral compositions. Furthermore, more data from similar projects should be collected to improve and expand the initial database, and the data should be continuously screened and analyzed to develop more universal equations.

Acknowledgments

This research described in this paper were financially supported by the National Funds for Distinguished Young scientists of China (No. 52125904) and Young Scientist Fund (No. 52309171).

References

Bruland, A. (1998), Hard Rock Tunnel Boring [Doctorate Thesis]. Norwegian University of Science and Technology, Trondheim, Norway.

Delisio, A. and Zhao, J. (2014), "A new model for TBM performance prediction in blocky rock conditions", *Tunn. Undergr. Sp. Tech.*, **43**, 440-452. https://doi.org/10.1016/j.tust.2014.06.004

Ewendt, G. (1989), Erfassung der Gesteinsabrasivität und Prognose des Werkzeugverschleißes beim maschinellen Tunnelvortrieb mit Diskenmeißeln. Bochumer geol. u. geot. Arbeiten 33. Bochum.

Frenzel, C. (2011), "Disc cutter wear phenomenology and their implications on disc cutter consumption for TBM", *Proceedings of the 45th US Rock Mechanics/Geomechanics Symposium*, San Francisco.

Gehring, K. (1995), "Prognosis of advance rates and wear for underground mechanized excavations", *Felsbau.*, **13**(6), 439-448. (in German).

Gong, Q.M. and Zhao, J. (2009), "Development of a rock mass characteristics model for TBM penetration rate prediction", *Int. J. Rock Mech. Min. Sci.*, **46**, 8-18. https://doi:10.1016/j.ijrmms.2008.03.003.

Gong, Q.M., Yin, L.J., Ma, H.S. and Zhao, J. (2016), "TBM tunnelling under adverse geological conditions: An overview", *Tunn. Undergr. Sp. Tech.*, **57**, 4-17. https://doi.org/10.1016/j.tust.2016.04.002

Kim, K.Y., Jo, S.A., Ryu, H.H. and Cho, G.C. (2020), "Prediction of TBM performance based on specific energy", *Geomech. Eng.*, **22**(6), 489-496. https://doi.org/10.12989/gae.2020.22.6.489.

Hassanpour, J., Rostami, J., Khamehchiyan, M., Bruland, A. and Tavakoli, H.R. (2010), "TBM performance analysis in pyroclastic rocks: A case history of Karaj water conveyance tunnel", *Rock Mech. Rock Eng.*, **43**(4), 427-445. https://doi.org/10.1007/s00603-009-0060-2.

Hassanpour, J., Rostami, J. and Zhao, J. (2011), "A new hard rock TBM performance prediction model for project planning", *Tunn. Undergr. Sp. Tech.*, **26**, 595-603. https://doi.org/10.1016/j.tust.2011.04.004.

Hassanpour, J., Rostami, J., Azali, S.T. and Zhao, J. (2014), "Introduction of an empirical TBM cutter wear prediction model for pyroclastic and mafic igneous rocks; a case history of Karaj water conveyance tunnel, Iran", *Tunn. Undergr. Sp. Tech.*, **43**, 222-231. https://doi.org/10.1016/j.tust.2014.05.007.

He, M.M., Zhang, Z.Q., Zheng, J., Chen, F.F. and Li, N. (2020), "A new perspective on the constant m(i) of the hoek-brown failure criterion and a new model for determining the residual strength of rock", *Rock Mech. Rock Eng.*, **53**(9), 3953-3967. https://doi.org/10.1007/s00603-020-02164-6.

ISRM (1979), "Suggested methods for determining the uniaxial compressive strength and deformability of rock materials", *Int. J. Rock Mech. Min. Sci. Geomech.*, **16**, 135-140.

Jeon, Y.J. and Lee, C.J. (2023), "Analysis of pile group behaviour to adjacent tunnelling considering ground reinforcement conditions with assessment of stability of superstructures", *Geomech. Eng.*, **33**(5), 463-475. https://doi.org/10.12989/gae.2023.33.5.463.

Karami, M., Zare, S. and Rostami, J. (2020), "Study of common wear prediction models for hard rock TBM disc cutters and comparison with field observation in Kerman water conveyance tunnel", *Bull. Eng. Geol. Environ.*, **80**(3), 1467-1476. https://doi.org/10.1007/s10064-020-01987-5.

Ko, T.Y., Kim, T.K., Son, Y. and Jeon, S. (2016), "Effect of geomechanical properties on Cerchar Abrasivity Index (CAI) and its application to TBM tunneling", *Tunn. Undergr. Sp. Tech.*, **57**, 99-111. https://doi.org/10.1016/j.tust.2016.02.006.

Lan, H., Xia, Y.M., Ji, Z.Y., Fu, J. and Miao, B. (2019), "Online monitoring device of disc cutter wear–design and field test", *Tunn. Undergr. Sp. Tech.*, **89**, 284-294. https://doi.org/10.1016/j.tust.2019.04.010.

Lan, H., Xia, Y.M., Miao, B., Fu, J. and Ji, Z.Y. (2020), "Prediction model of wear rate of inner disc cutter of engineering in Yinsong, Jilin", *Tunn. Undergr. Sp. Technol.*, **99**, 103338. https://doi.org/10.1016/j.tust.2020.103338.

Li, X.C., Li, X.G. and Yuan, D.J. (2017), "Application of an interval wear analysis method to cutting tools used in tunneling shields in soft ground", *Wear.*, **392-393**, 21-28. https://doi.org/10.1016/j.wear.2017.09.010.

Li, J.B., Jing, L.J. Zheng, X.F., Li, P.Y. and Yang, C. (2019), "Application and outlook of information and intelligence technology for safe and efficient TBM construction", *Tunn. Undergr. Sp. Tech.*, **93**, 103097. https://doi.org/10.1016/j.tust.2019.103097.

Li, Y.L., She, L., Wen, L.F. and Zhang, Q. (2020), "Sensitivity Analysis of Drilling Parameters in Rock Rotary Drilling Process Based on Orthogonal Test Method", *Eng. Geol.*, **270**, 105576. https://doi.org/10.1016/j.enggeo.2020.105576.

Li, Y.H., Tang, X.J., Yang, S. and Ding, Y.F. (2023), "Characterization of face stability of shield tunnel excavated in sand-clay mixed ground through transparent soil models", *Geomech. Eng.*, **33**(5), 439-451. https://doi.org/10.12989/gae.2023.33.5.439.

Ling, X.Z., Kong, X.X., Tang, L., Cong, S.Y. and Tang, W.C. (2022), "Preliminary identification of potential failure modes of a disc cutter in soil-rock compound strata: Interaction analysis and case verification", *Eng. Fail. Anal.*, **138**, 105907. https://doi.org/10.1016/j.engfailanal.2021.105907.

Liu, Q.S., Huang, X., Gong, Q.M., Du, L.J., Pan, Y.C. and Liu, J.P. (2016), "Application and development of hard rock TBM and its prospect in China", *Tunn. Undergr. Sp. Tech.*, **57**, 33-46. https://doi.org/10.1016/j.tust.2016.01.034.

Liu, Q.S., Liu, J.P., Pan, Y.C., Zhang, X.P., Peng, X.X., Gong, Q.M. and Du, L.J. (2017), "A wear rule and cutter life prediction model of a 20-in. TBM cutter for granite: a case study of a water conveyance tunnel in China", *Rock Mech. Rock*

Eng., **50**, 1303-1320. https://doi.org/10.1007/s00603-017-1176-4.

Rabinowicz, E. (1995), Friction and wear of materials, John Wiley & Sons.

Ren, D.J., Shen, S.L., Arulrajah, A. and Cheng, W.C. (2018), "Prediction model of TBM disc cutter wear during tunneling in heterogeneous ground", *Rock Mech. Rock Eng*., **51**, 3599-3611. https://doi.org/10.1007/s00603-018-1549-3.

Rostami, J. (1997), Development of a force estimation model for rock fragmentation with disc cutters through theoretical modeling and physical measurement of crushed zone pressure[Doctorate Dissertation][D]. Golden, Colorado, USA: Colorado School of Mines.

Rostami, J. (2013), "Study of pressure distribution within the crushed zone in the contact area between rock and disc cutters", *Int. J. Rock Mech. Min. Sci*., **57**(1), 172-186. https://doi.org/10.1016/j.ijrmms.2012.07.031.

She, L., Zhang, S.R., Wang, C., Du, M. and Yang, P. (2022a), "A cutting mechanics model of constant cross-section type disc cutter and its application based on dense core theory", *Int J Rock Mech Min Sci.*, **150**, 105025. https://doi.org/10.1016/j.ijrmms.2021.105025.

She, L., Zhang, S.R., Wang, C., Wu, Z.Q., Yu, L.C. and Wang, L.X. (2022b), "Prediction model for disc cutter wear during hard rock breaking based on plastic removal abrasiveness mechanism", *Bull. Eng. Geol. Environ.*, **81**, 432. https://doi.org/10.1007/s10064-022-02915-5.

She, L., Zhang, S.R., He, S.W., Wang, C., Li, L., Jing, Y. and Liu, Y. (2022c), "Investigation on wear prediction model of TBM disc cutter based on dense core theory", *Chin. J. Geotech. Eng*., **44**(5), 1-7. (in Chinese).

She, L., Zhang, S.R., Wang, C., Li, Y.L. and Du, M. (2023), "A new method for wear estimation of TBM disc cutter based on energy analysis", *Tunn. Undergr. Sp. Tech*., **131**, 104840. https://doi.org/10.1016/j.tust.2022.104840.

Shen, X., Yuan, D., Lin, X.T., Chen, X. and Peng, Y. (2022), "Evaluation and prediction of earth pressure balance shield performance in complex rock strata: A case study in Dalian, China". *J. Rock Mech. Geotech. Eng*., **15**(6), 1491-1505. https://doi.org/10.1016/j.jrmge.2022.09.010.

Su, W.L., Li, X.G., Jin, D.L., Yang, Y., Qin, R.C. and Wang, X.Y., (2020), "Analysis and prediction of TBM disc cutter wear when tunneling in hard rock strata: A case study of a metro tunnel excavation in Shenzhen, China", *Wear*., **446–447**, 203190. https://doi.org/10.1016/j.wear.2020.203190.

Sun, Z.C., Zhao, H.L., Hong, K.R., Chen, K., Zhou, J.J., Li, F.Y., Zhang, B., Song, F.L., Yang, Y.D. and He, R.Y. (2019), "A practical TBM cutter wear prediction model for disc cutter life and rock wear ability", *Tunn. Undergr. Sp. Tech*., **85**, 92-99. https://doi.org/10.1016/j.tust.2018.12.010.

Sun, R.X., Mo, J.L., Zhang, M.Q., Su, Y.M. and Zhou, Z.R. (2022), "Cutting performance and contact behavior of partial-wear TBM disc cutters: A laboratory scale investigation", *Eng. Fail. Anal*., **137**, 106253. https://doi.org/10.1016/j.engfailanal.2022.106253.

The National Standards Compilation Group of People's Republic of China GB/T50218–2014. Standard for Engineering Classification of Rock Masses. China Planning Press, Beijing, p. 84 (in Chinese).

Wan, Z.C., Sha, M.Y. and Zhou, Y.L. (2002a), "Study on disk cutters for hard rock (1), application of TB880E TBM in Qinling Tunnel", *Modern. Tunn Technol*., **39**(5), 1-11. (in Chinese).

Wan, Z.C., Sha, M.Y. and Zhou, Y.L. (2002b), "Study on disk cutters for hard rock (2), application of TB880E TBM in Qinling Tunnel", *Modern. Tunn Technol*., **39**(6), 1-12. (in Chinese).

Wang, L.H., Kang, Y.L., Zhao, X.J. and Zhang, Q. (2015), "Disc cutter wear prediction for a hard rock TBM cutterhead based on energy analysis", *Tunn. Undergr. Sp. Tech*., **50**, 324-333. https://doi.org/10.1016/j.tust.2015.08.003.

Wang, F., Men, C.H., Kong, X.W. and Meng, L.X. (2019), "Optimum design and application research of Eddy current sensor for measurement of TBM disc cutter wear", *Sensors*., **19**(19), 4230. https://doi.org/10.3390/s19194230.

Yang, J.H., Zhang, X.P., Ji. P.Q., Liu, Q.S., Lu, X.J., Wei, J.P., Qi, S.H., Fang, H.G., Fang, J.N. and Geng, Y.J. (2019), "Analysis of disc cutter damage and consumption of TBM1 section on water conveyance tunnel at Lanzhou water source construction engineering", *Tunn. Undergr. Sp. Tech*., **85**, 67-75. https://doi.org/10.1016/j.tust.2018.11.040.

Yu, H.G., Tao, J.F., Huang, S., Qin, C.J., Xiao, D.Y. and Liu, C.L. (2021), "A field parameters-based method for real-time wear estimation of disc cutter on TBM cutterhead", *Automat. Constr*., **124**, 103603. https://doi.org/10.1016/j.autcon.2021.103603.

Zhang, G., Tan, J., Zhang, L. and Xiang, Y. (2015), "Linear regression analysis for factors influencing displacement of high-filled embankment slopes", *Geomech. Eng*., **8**(4), 511-521. https://doi.org/10.12989/gae.2015.8.4.511.

Zhang, S.R., She, L., Wang, C., Wang, Y.J., Cao, R.L., Li, Y.L. and Cao, K.L. (2021), "Investigation on the relationship among the Cerchar abrasivity index, drilling parameters and physical and mechanical properties of the rock", *Tunn. Undergr. Sp. Tech*., **112**, 103907. https://doi.org/10.1016/j.tust.2021.103907.

Zhao, H.M., Shu, B., Xia, Y.M. and Zheng, W. (2014), "Study of wear prediction for TBM cutter based on abrasive wear model", *J. Rail. Sci. Eng*., **11**(8), 152-158. (in Chinese).

Zhou, W., Li, S.L., Ma, G., Chang, X.L., Cheng, Y.G. and Ma, X. (2016), "Assessment of the crest cracks of the Pubugou rockfill dam based on parameters back analysis", *Geomech. Eng*., **11**(4), 571-585. https://doi.org/10.12989/gae.2016.11.4.571.

CC